Electronic Supplementary Material (ESI) for Journal of Materials Chemistry C.

Supporting Information for

Near infrared-to-blue photon upconversion by exploiting direct S-T absorption of a molecular sensitizer

Yoichi Sasaki,[a] Shogo Amemori,[a] Hironori Kouno,[a] Nobuhiro Yanai,*[a,b] and Nobuo Kimizuka*[a]

[a]Department of Chemistry and Biochemistry, Graduate School of Engineering, Center for Molecular Systems (CMS), Kyushu University, 744 Moto-oka, Nishi-ku, Fukuoka 819-0395, Japan.

[b]PRESTO, JST, Honcho 4-1-8, Kawaguchi, Saitama 332-0012, Japan.

E-mail: yanai@mail.cstm.kyushu-u.ac.jp; n-kimi@mail.cstm.kyushu-u.ac.jp.

Materials.

All reagents and solvents were used as received without further purification otherwise noted. Osmium(III) chloride hydrate, ammonium hexafluorophosphate and poly(vinyl alcohol) were purchased from Sigma-Aldrich. 4'-(4-bromophenyl)-2,2':6',2''-terpyridine, 2,5,8,11-tetra-*tert*-butylperylene (TTBP) were purchased from TCI. TTBP was purified through recrystallization with acetonitrile.

Synthesis of Os(bptpy)$_2^{2+}$.

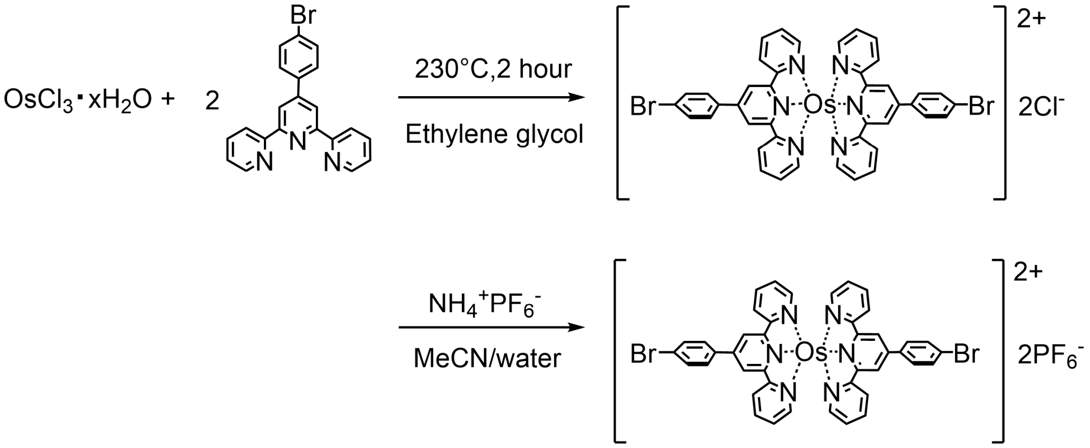

Osmium(III) chloride hydrate (89.4 mg, ca. 0.30 mmol) and 4'-(4-bromophenyl)-2,2':6',2''-terpyridine (234.6 mg, 0.60 mmol) were refluxed in ethylene glycol for 2 hours at 230 ˚C using microwave (Biotage Initiator 2.5) under continuous stirring. Dark purple solution was obtained. After cooling to room temperature, deionized water (10 mL) was added, giving dark purple precipitates. The precipitates were filtrated and washed with water and THF. The product was dissolved in acetonitrile (80 mL) and heated at 70 °C. Aqueous solution (20 mL) of ammonium hexafluorophosphate (2 g, 12.3 mmol) was added under stirring, resulting in dark purple precipitates. The residue was recrystallized with acetonitrile. ^{1}H NMR (400 MHz, DMSO-d_6, TMS): δ (ppm) 7.21 (t, J = 6.8, 6.4 Hz, 4H), 7.43 (d, J = 5.6 Hz, 4H), 7.93-8.01 (m, 8H), 8.38 (d, J = 8.4 Hz, 4H), 9.09 (d, J = 8.4 Hz, 4H), 9.52 (s, 4H).^{13}C NMR (400 MHz, DMSO-d_6, TMS): δ (ppm) 119.5, 124.1, 124.9, 127.9, 129.8, 132.0, 134.5, 137.7, 144.6, 152.2, 154.6, 159.5. MS (MALDI): m/z = 965 ([M–2PF$_6^-$–H]$^+$), 887 ([M–2PF$_6^-$–Br]$^+$). Elemental analysis: calculated for $C_{42}H_{28}Br_2N_6F_{12}P_2Os$: C 40.14 H 2.25 N 6.69, Found C 40.17 H 2.25 N 6.62.

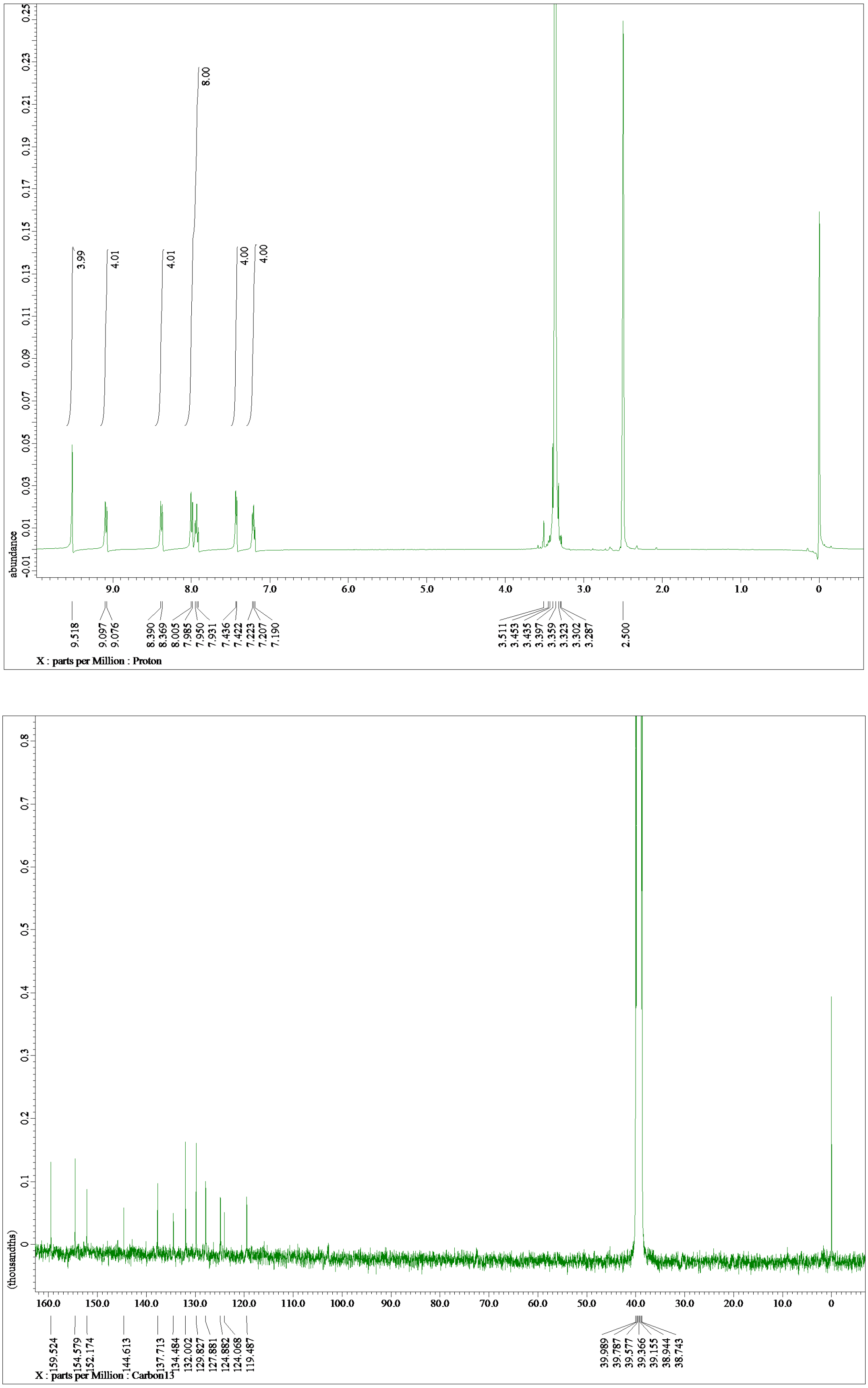

^{1}H NMR (top) and ^{13}C NMR (bottom) spectra (400 MHz, DMSO-d_6, TMS) of Os(bptpy)$_2^{2+}$.

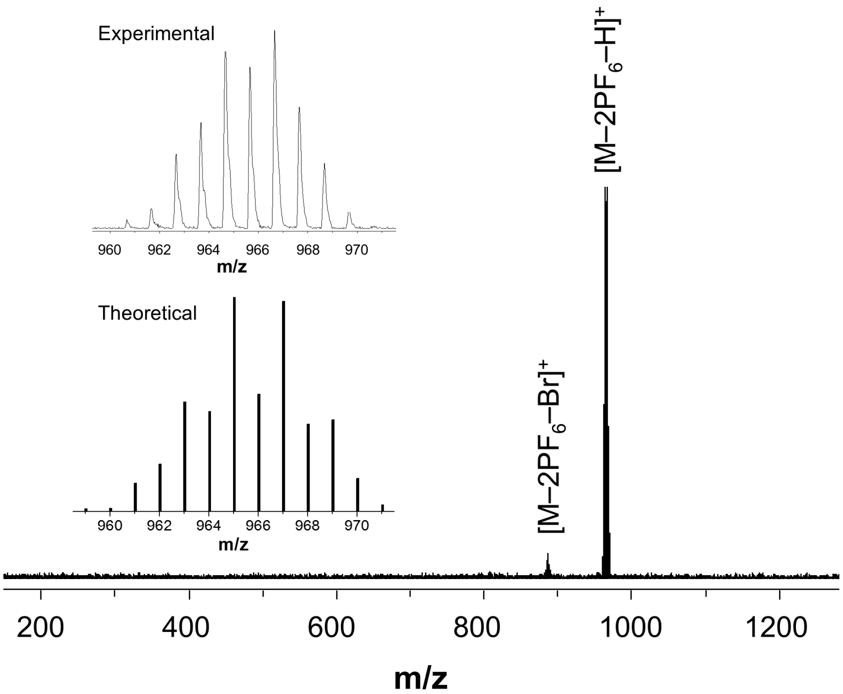

Mass spectrum of $Os(bptpy)_2^{2+}$. Inset: experimental and theoretical distributions for $[M - 2PF_6 - H]^+$.

Characterizations.

^{1}H NMR and ^{13}C NMR (400 MHz) spectra were measured on a JEOL JNM-ECZ400S. Mass spectroscopy analysis was conducted on a Bruker Autoflex III. Elemental analysis was conducted at the Elemental Analysis Center, Kyushu University. Absorption spectra were recorded on a JASCO V-670 spectrophotometer. Fluorescence spectra were measured by using a PerkinElmer LS 55 fluorescence spectrometer. The samples were excited at an incidence angle of 45° to the quartz cell surface, and the fluorescence was detected along the normal.

For TTA-UC emission measurements, a diode laser (724 nm, 40 mW, RGB Photonics) was used as an excitation source. The laser power was controlled by combining a software (Ltune) and a variable neutral density filter, and measured using a PD300-UV photodiode sensor (OPHIR Photonics). The laser beam was focused on a sample using a lens. The diameter of laser beam (1/e^{2}) was measured at the sample position using a CCD beam profiler SP620 (OPHIR Photonics). The typical irradiation area was 9.1×10^{-5} cm^{-2}. The emitted light was collimated by an achromatic lens, the excitation light was removed using a 610 nm short-pass filter (Asahi Spectra), and the emitted light was again focused by an achromatic lens to an optical fiber connected to a multichannel detector MCPD-9800 (Otsuka Electronics).

Time-resolved photoluminescence lifetime measurements were carried out by using a time-correlated single photon counting lifetime spectroscopy system, HAMAMATSU Quantaurus-Tau C11367-02 (for fluorescence and phosphorescence lifetime)/C11567-01(for delayed luminescence lifetime). X-ray powder diffraction (XRPD) analysis was conducted on a BRUKER D2 PHASER with a Cu Kα source (λ = 1.5418 Å). The UC quantum yield of solid samples were determined by an absolute quantum yield measurement system in an integrating sphere using a laser excitation source and a calibrated spectrometer specially built by Hamamatsu Photonics.

Determination of TTA-UC quantum yield.

The upconverted luminescence quantum efficiency in deaerated DMF was determined relative to a standard, Os(bptpy)$_2^{2+}$ in deaerated DMF (20 μM), according to the following equation.

$$\Phi_{\mathrm{UC}}' = 2\Phi_{\mathrm{std}}\left(\frac{A_{\mathrm{std}}}{A_{\mathrm{UC}}}\right)\left(\frac{I_{\mathrm{std}}}{I_{\mathrm{UC}}}\right)\left(\frac{F_{\mathrm{UC}}}{F_{\mathrm{std}}}\right) \tag{S1}$$

Where Φ, A, I, and F represent the quantum yield, absorbance at 724 nm, excitation intensity, and integrated photoluminescence spectral profile. The subscripts UC and std denote the parameters of the upconversion and standard systems. Note that the theoretical maximum of Φ_{UC}' is standardized to be 1 (100%). For the estimation of Φ_{std} and F_{std}, the emission in the range from 750 nm to 930 nm was used because of the wavelength overlap of excitation (724 nm) with emission.

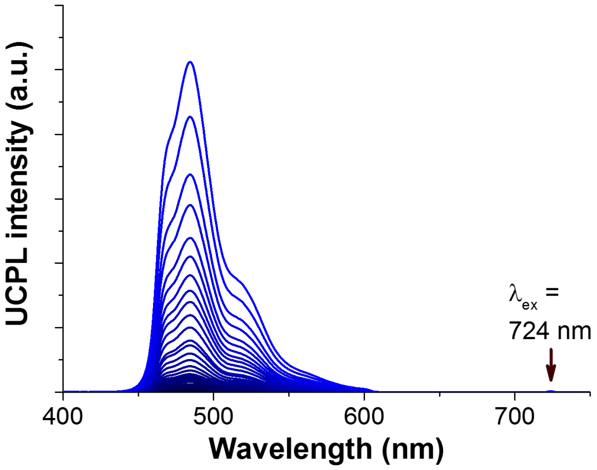

Figure S1. PL spectra of Os(bptpy)$_2^{2+}$-TTBP in deaerated DMF ([Os(bptpy)$_2^{2+}$] = 20 μM, [TTBP] = 20 mM) with various excitation intensities from 21.9 mW cm^{-2} to 11.0 W cm^{-2} (λ_{ex} = 724 nm, 610 nm short pass filter). By increasing the TTBP concentration from 2 mM (Fig. 2b) to 20 mM, the PL peak at 462 nm was partially suppressed. This is because the overlap of absorption and emission bands of TTBP (Fig. 2a) induces a self-absorption at such high concentration.

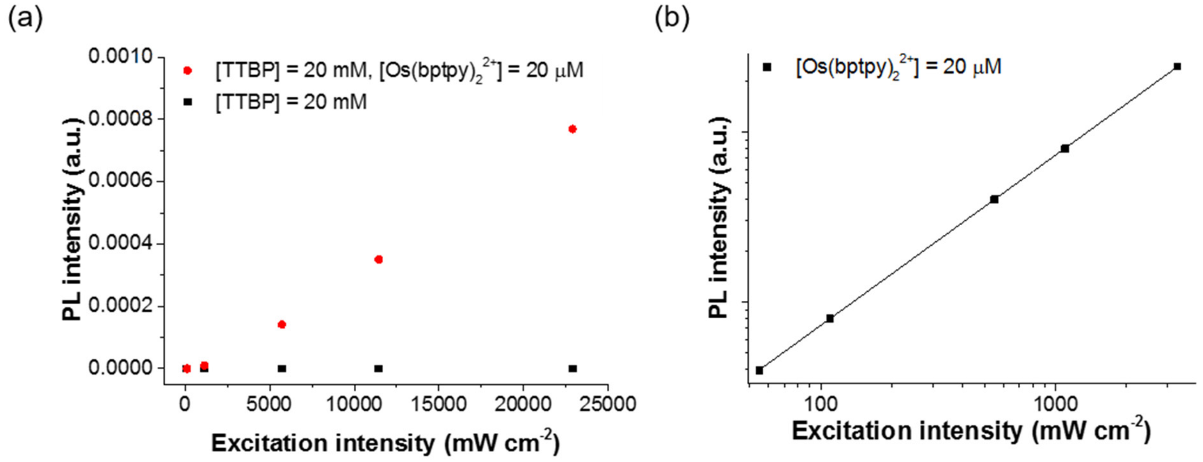

Figure S2. (a) Photoluminescence (PL) intensity at 484 nm of TTBP (black dots, [TTBP] = 20 mM, under Ar) and Os(bptpy)$_2^{2+}$-TTBP (red dots, [Os(bptpy)$_2^{2+}$] = 20 μM, [TTBP] = 20 mM, under Ar) under excitation at 724 nm. (b) Photoluminescence (PL) intensity at 742 nm of Os(bptpy)$_2^{2}$ ([Os(bptpy)$_2^{2+}$] = 20 μM, under Ar) under excitation at 724 nm. The linear fit of the data gave a slope of 1.

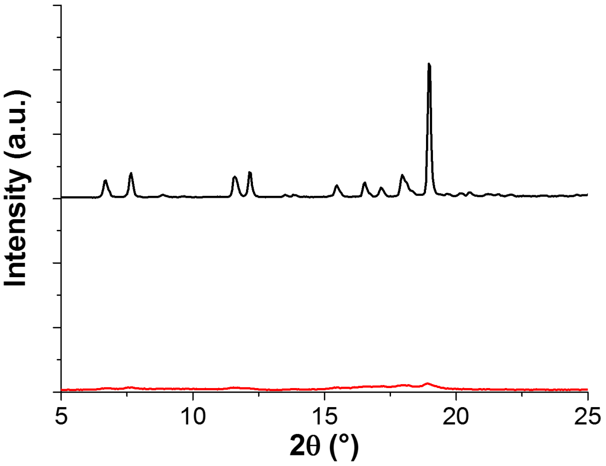

Figure S3. X-ray powder diffraction (XRPD) patterns of Os(bptpy)$_2^{2+}$-TTBP (Os(bptpy)$_2^{2+}$/TTBP = 0.5 mol%) before (black) and after (red) mechanical grinding in the solid state. Peak weakening by grinding indicates the decreased crystallinity of the material.

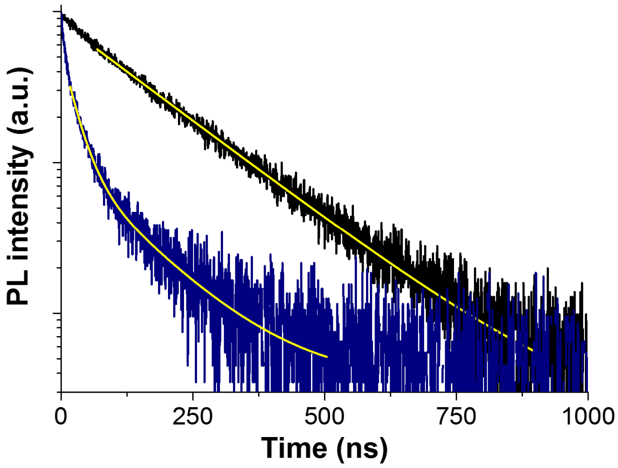

Figure S4. Phosphorescence decays of Os(bptpy)$_2^{2+}$ (black) and Os(bptpy)$_2^{2+}$-TTBP (blue, Os(bptpy)$_2^{2+}$/TTBP = 0.5 mol%) in PVA film (λ_{ex} = 470 nm, λ_{em} = 742 nm). The Os(bptpy)$_2^{2+}$ in PVA was prepared in the similar way to Os(bptpy)$_2^{2+}$-TTBP in PVA. The Os(bptpy)$_2^{2+}$ in PVA showed a single-exponential decay with a phosphorescence lifetime of 166 ns. The phosphorescence of Os(bptpy)$_2^{2+}$-TTBP pair apparently decayed faster than that of Os(bptpy)$_2^{2+}$, and it could be fitted as a double-exponential decay with an averaged lifetime of 26 ns. Notable decrease of τ_P implies an efficient TTET from Os(bptpy)$_2^{2+}$ to neighboring TTBP in the condensed state.

Table S1. Fluorescence quantum yield Φ_F of TTBP with different TTBP and $Os(bptpy)_2^{2+}$ concentrations (λ_{ex} = 414 nm).

	Φ_F ([TTBP] = 2 mM)	Φ_F ([TTBP] = 20 mM)
[$Os(bptpy)_2^{2+}$] = 0 μM	94%	85%
[$Os(bptpy)_2^{2+}$] = 20 μM	52%	50%

In the absence of donor $Os(bptpy)_2^{2+}$, a drop of Φ_F from 94% to 85% was observed by increasing the TTBP concentration from 2 mM to 20 mM, which would be due to the re-absorption. Note that the Φ_F value of TTBP at a lower concentration ([TTBP] = 20 μM) was similar (92%) to the one at 2 mM (94%). The fluorescence lifetime of TTBP was almost similar between 2 mM (6.3 ns) and 20 mM (6.4 ns), implying the very small effect of concentration quenching for TTBP. Rather, it is more likely that the re-absorption of acceptor fluorescence occur with different molecules.

By adding 20 μM donor $Os(bptpy)_2^{2+}$, the Φ_F value significantly decreased from 94% to 52% ([TTBP] = 2 mM) and from 85% to 50% ([TTBP] = 20 mM). This is reasonable considering the spectral overlap between acceptor emission and donor absorption (Fig. 2a). Here, the acceptor-to-donor singlet-singlet back energy transfer has almost no contribution since the fluorescence lifetime of TTBP was not affected by the presence of donor (6.2 ns for [$Os(bptpy)_2^{2+}$] = 20 μM, [TTBP] = 20 mM). Consistently with the above discussion, the efficiency of fluorescence re-absorption by donor and acceptor ($\Phi_{Re} = \Phi_F/\Phi_{F0}$, Φ_{F0} = 94%) was not affected by the concentration of TTBP (55% and 53% for [TTBP] = 2 mM and 20 mM, respectively).

Meanwhile, the TTET efficiency was increased for 3.9 times (from 12% to 47%, Fig. 2d) by increasing the TTBP concentration from 2 mM to 20 mM. This increment ratio is close to that of UC quantum yield by increasing the acceptor concentration (3.8 times). These results suggest that the improvement of UC quantum yield is mainly due to the improved donor-to-acceptor TTET efficiency.